

1           **A transcriptome based molecular classification scheme for**  
2           **cholangiocarcinoma and subtype derived prognostic biomarker**

3    **Authors**

4    Zhongqi Fan<sup>1, #</sup>, Xinchun Zou<sup>2, #</sup>, Guangyi Wang<sup>1</sup>, Yahui Liu<sup>1</sup>, Yanfang Jiang<sup>3</sup>,  
5    Haoyan Wang<sup>2</sup>, Ping Zhang<sup>1</sup>, Feng Wei<sup>1</sup>, Xiaohong Du<sup>1</sup>, Meng Wang<sup>1</sup>,  
6    Xiaodong Sun<sup>1</sup>, Bai Ji<sup>1</sup>, Xintong Hu<sup>3</sup>, Liguang Chen<sup>3</sup>, Peiwen Zhou<sup>3</sup>, Duo Wang<sup>3</sup>,  
7    Jing Bai<sup>2</sup>, Xiao Xiao<sup>4</sup>, Lijiao Zuo<sup>2</sup>, Xuefeng Xia<sup>2</sup>, Xin Yi<sup>2, 5</sup>, Guoyue Lv<sup>1, \*</sup>

8

9    <sup>1</sup>Department of Hepatobiliary and Pancreatic Surgery, General Surgery  
10   Center, First Hospital of Jilin University, Changchun, China; <sup>2</sup>Geneplus-Beijing  
11   Institute, 9th Floor, No.6 Building, Peking University Medical Industrial Park,  
12   Zhongguancun Life Science Park, Beijing, China; <sup>3</sup>Genetic Diagnosis Center,  
13   The First Hospital of Jilin University, Changchun, China; <sup>4</sup>Geneplus-Shenzhen,  
14   No.14 Zhongxing Road, Pingshan District, Shenzhen, China; <sup>5</sup>School of  
15   Computer Science and Technology, Xi'an Jiaotong University, Xi'an, China;

16   <sup>#</sup>These authors contributed equally as co-first authors of this article.

17   <sup>\*</sup>Corresponding author

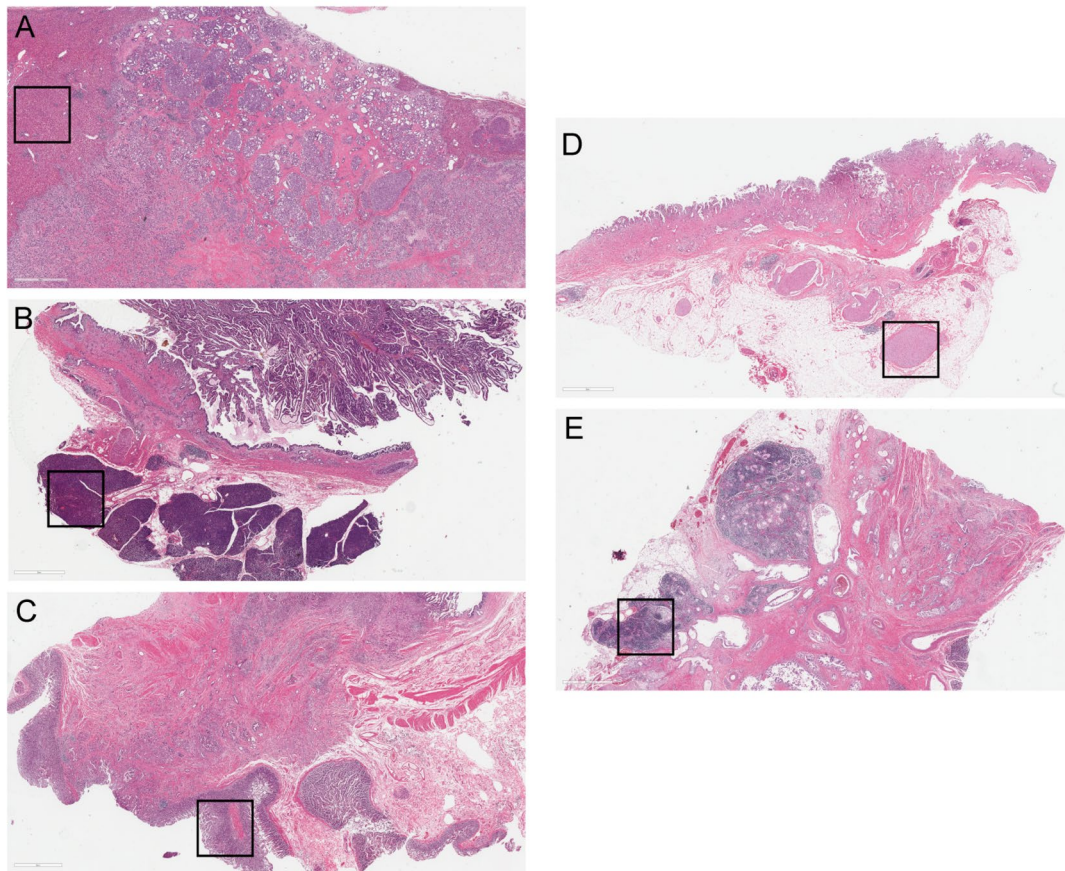
18   **Contents**

19   **Supplementary Figures: 16; pages 2-29.**

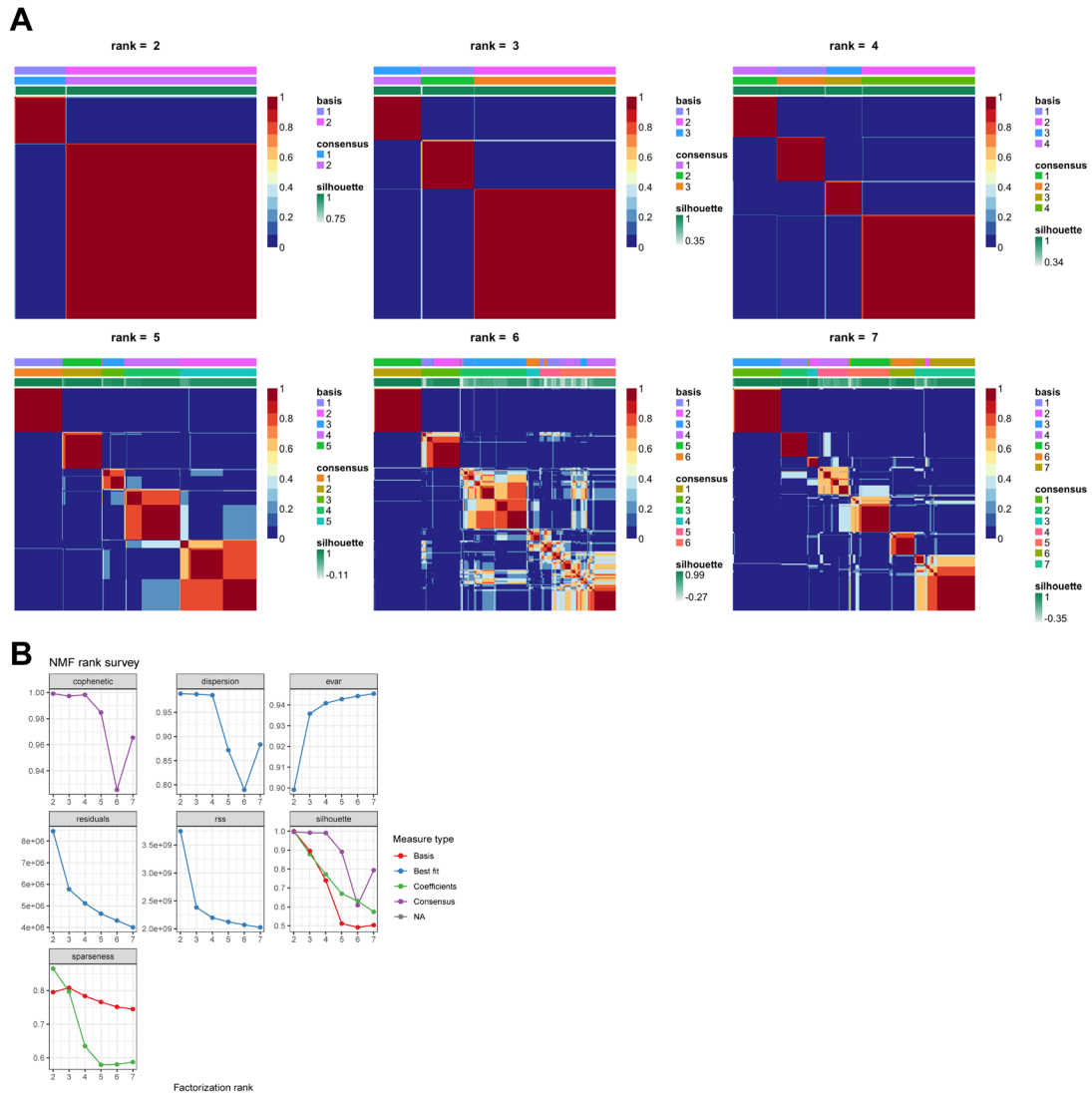
20   **Supplementary Tables: 10; pages 30-41.**

21

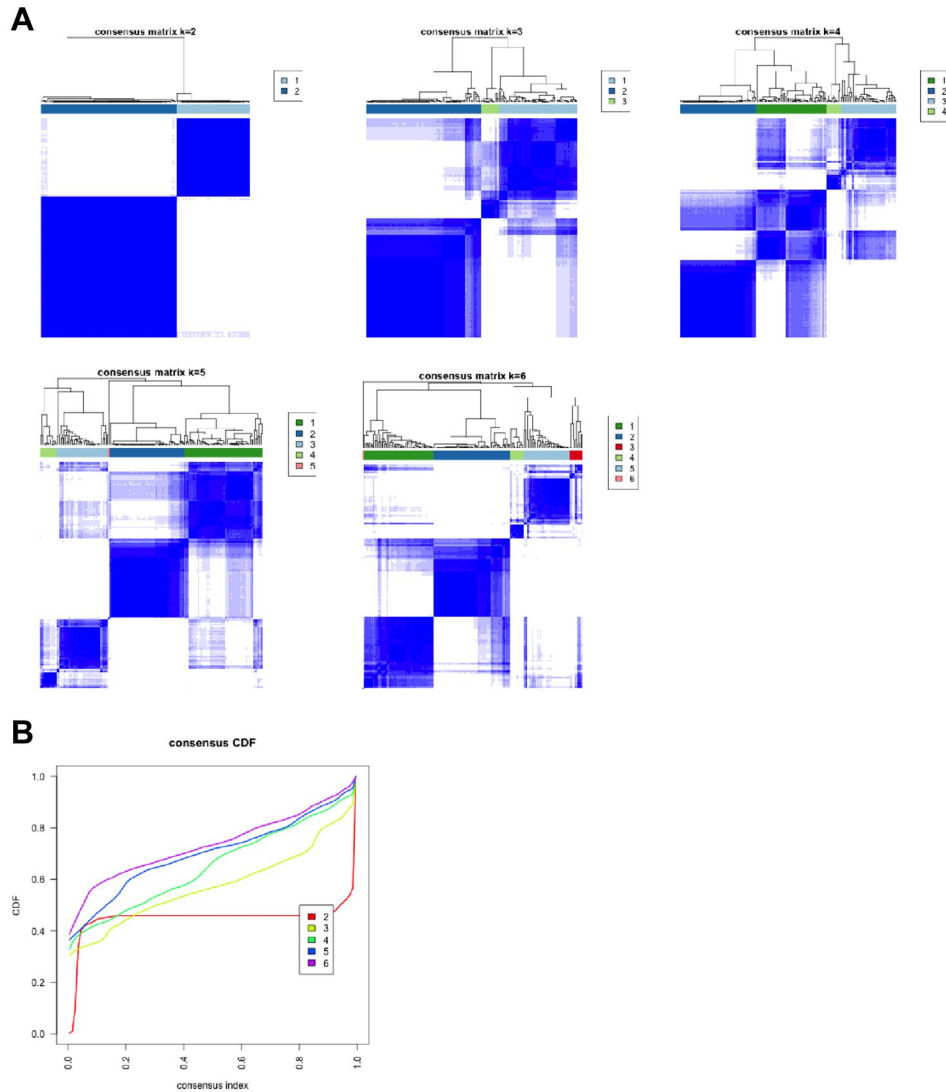
22 **Supplementary Figures**



23 **Supplementary Fig. 1. Normal tissue contamination of CCA tumor**  
24 **samples.** Representative images of H&E staining of hepatic (A), pancreatic  
25 (B), duodenal (C), neural (D) and lymphatic (E) tissues contamination. Bar, 2  
26 mm. Black box marks the normal tissue contamination.

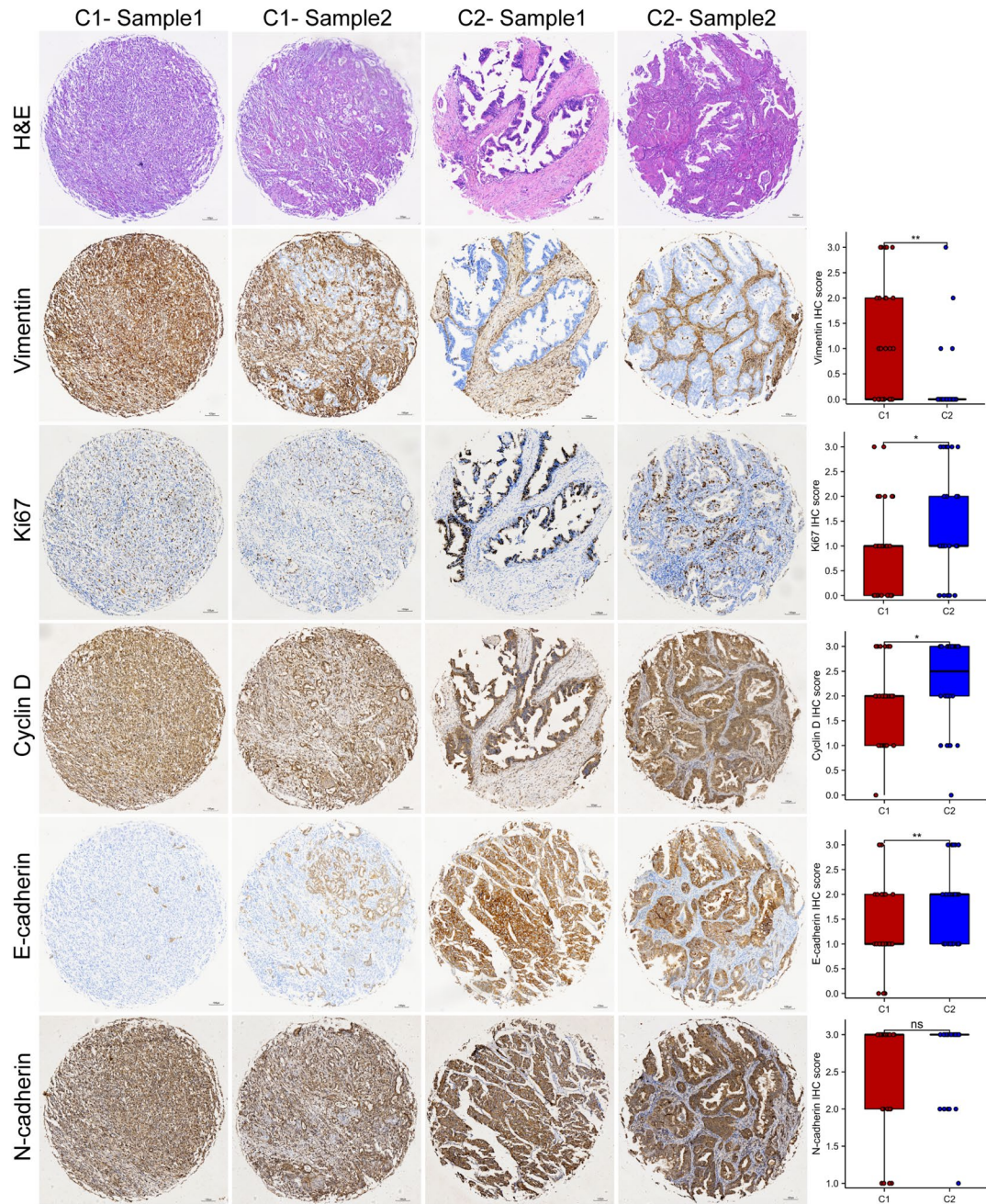


**Supplementary Fig. 2. Unsupervised classification of 438 CCAs by performing non-negative matrix factorization (NMF) on transcriptomic data. (A)** Heatmap displaying the classification solutions for  $k=2$  to  $k=7$  classes. **(B)** NMF rank survey representing the change of different parameter values with increasing  $k$ . The cophenetic coefficient for  $k=2$  and  $k=4$  was similarly high. As a solution for more classes was desired,  $k=4$  was considered as the best solution.



**Supplementary Fig. 3. Unsupervised classification of 164 CCAs by performing consensus clustering on transcriptomic data. (A)** Heatmap displaying the consensus matrix for  $K=2$  to  $K=6$  classes. **(B)** Empirical cumulative distribution functions (CDFs) corresponding to the entries of consensus matrices for  $K=2$  to  $K=6$ . As empirical cumulative distribution function for  $K=2$  was approximately constant with the increasing consensus index,  $K=2$  was considered as the best solution.

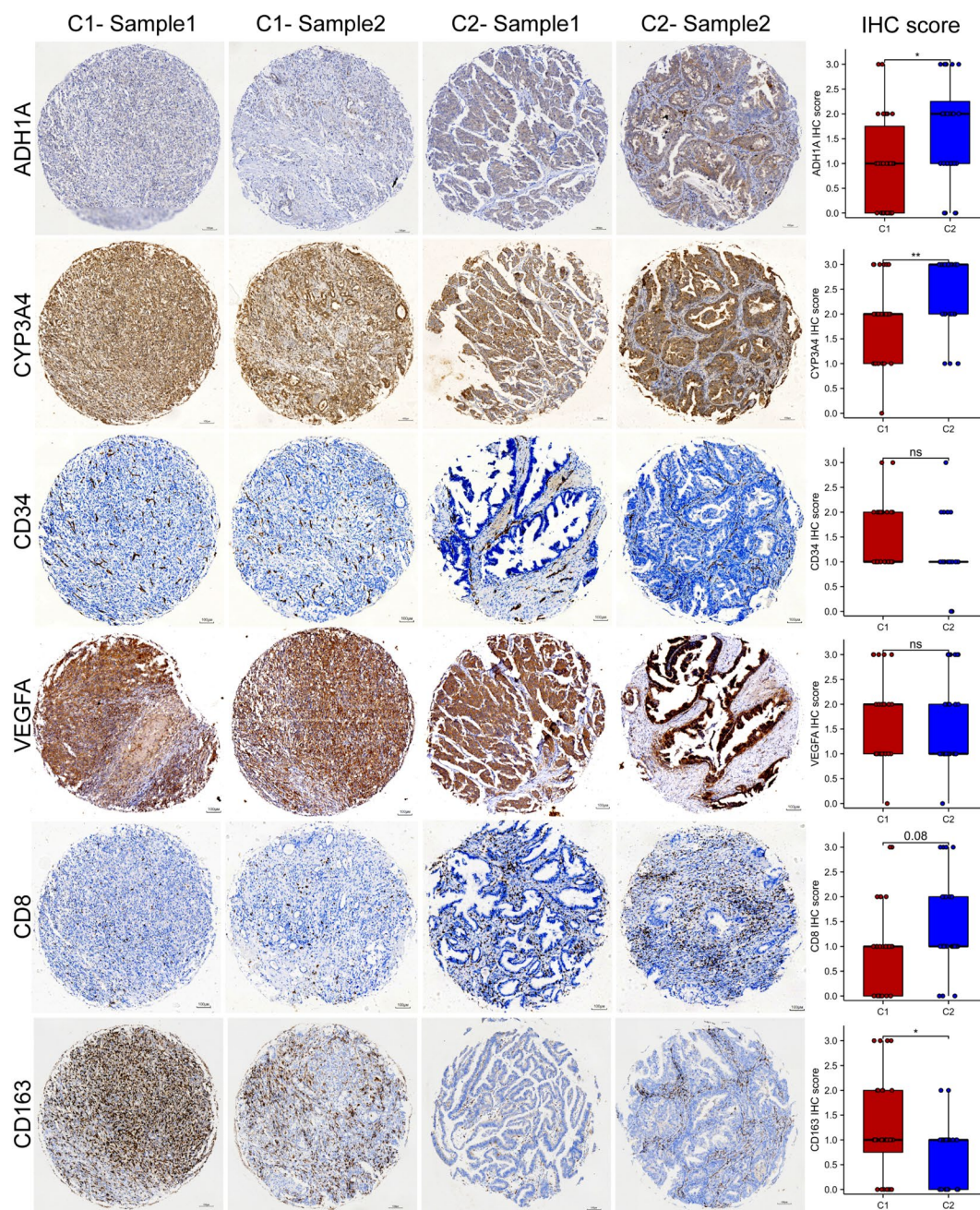




**Supplementary Fig. 4. Immunofluorescence showed different EMT and proliferation characteristics of each class. IHC staining of E-cadherin/Vimentin/N-cadherin showed the expression level of EMT core proteins. IHC staining of Ki67 and Cyclin D showed the expression level of proliferation-associated proteins. The histogram on the right shows the**

52 statistical results of each group staining. *P* values were calculated by two-  
53 sided Wilcoxon rank sum test. C1, n = 18; C2, n = 18.  
54

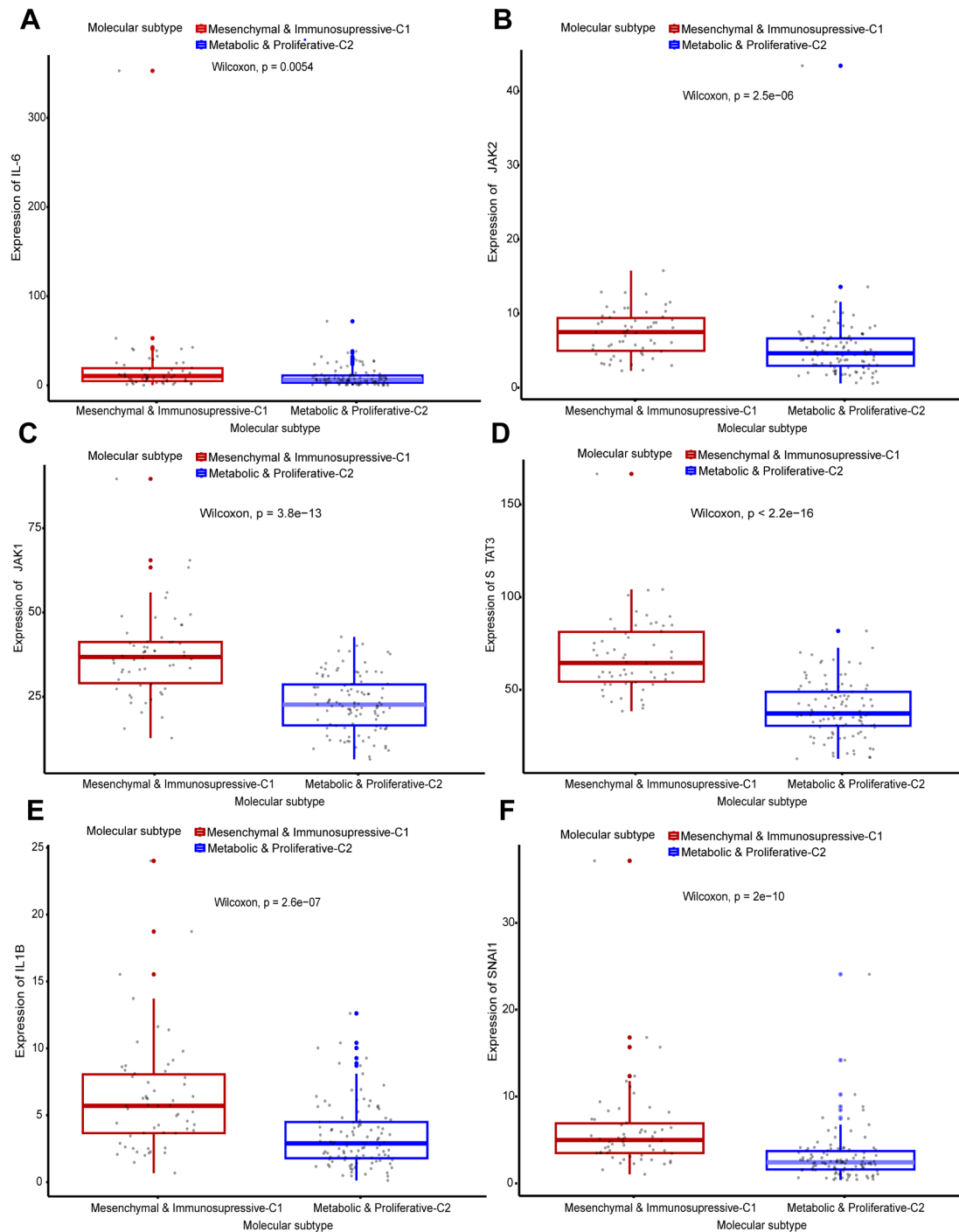




56

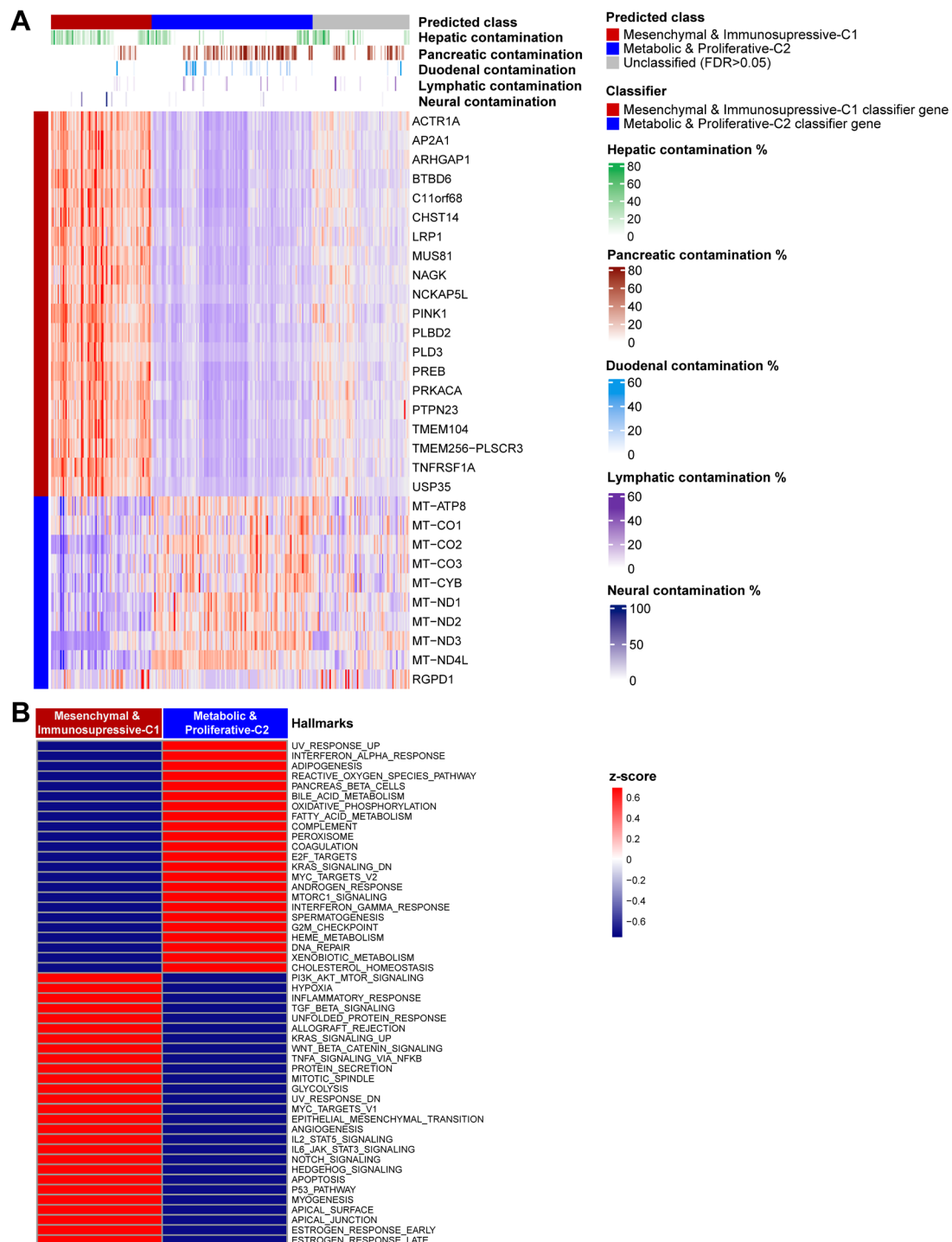
57 **Supplementary Fig. 5. Immunofluorescence showed different**58 **metabolic/angiogenesis/immune characteristics of each class. CYP3A4**59 **and ADH1A was used to characterize metabolic differences of each class.**60 **IHC staining of CD34 and VEGFA showed the expression level of**61 **angiogenesis key proteins. CD8 and CD163 were used to represent the**

62 infiltration of T cells and M2 macrophage, respectively. The histogram on the  
63 right shows the statistical results of each group staining. *P* values were  
64 calculated by two-sided Wilcoxon rank sum test. C1, n = 18; C2, n = 18.  
65



**Supplementary Fig. 6. Relative RNA level of genes associated with classical oncogenic signaling pathways in each class. Box plots representing the relative RNA expression of (A) *IL-6*; (B) *JAK2*; (C) *JAK1*; (D)**

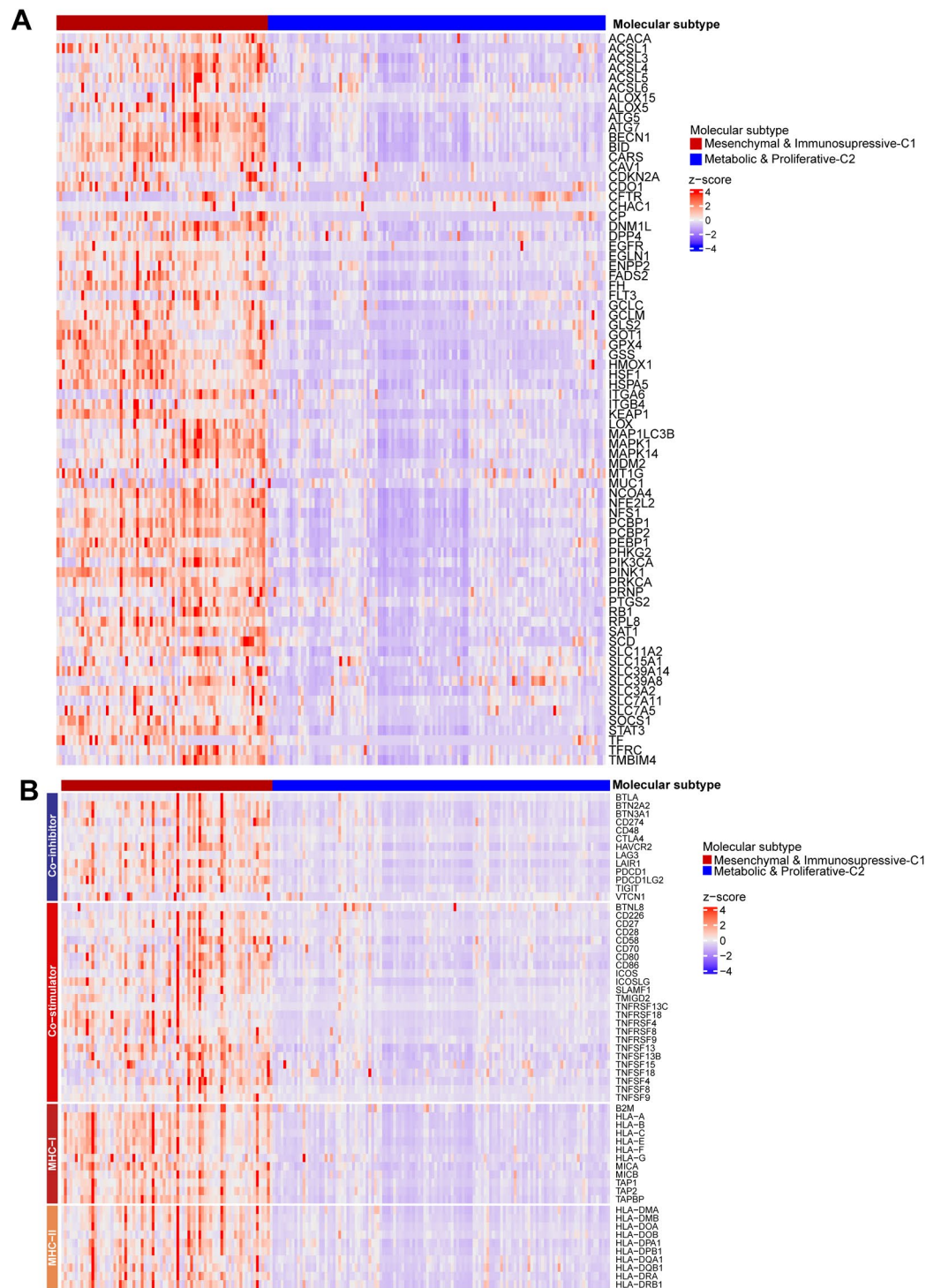
70 *STAT3*; (E) *IL-1B*; (F) *SNAI1*. *P* values were calculated by two-sided Wilcoxon  
71 rank sum test. C1, n = 58; C2, n = 108.



**Supplementary Fig. 7. Validation of classifier and molecular classification scheme on the verification cohort. (A)** Heatmap representing the expression of classifier genes in each sample (verification cohort, N=274). The expression levels were represented by normalized z-



77 scores. The molecular class was predicted by nearest template prediction  
78 (NTP) analysis. **(B)** Heatmap representing the enrichment of hallmark gene  
79 sets in molecular classes for the verification cohort. Single-sample gene set  
80 enrichment analysis (ssGSEA) was used to obtain enrichment scores, with  
81 samples from the same subtype indicated with a normalized z-score.



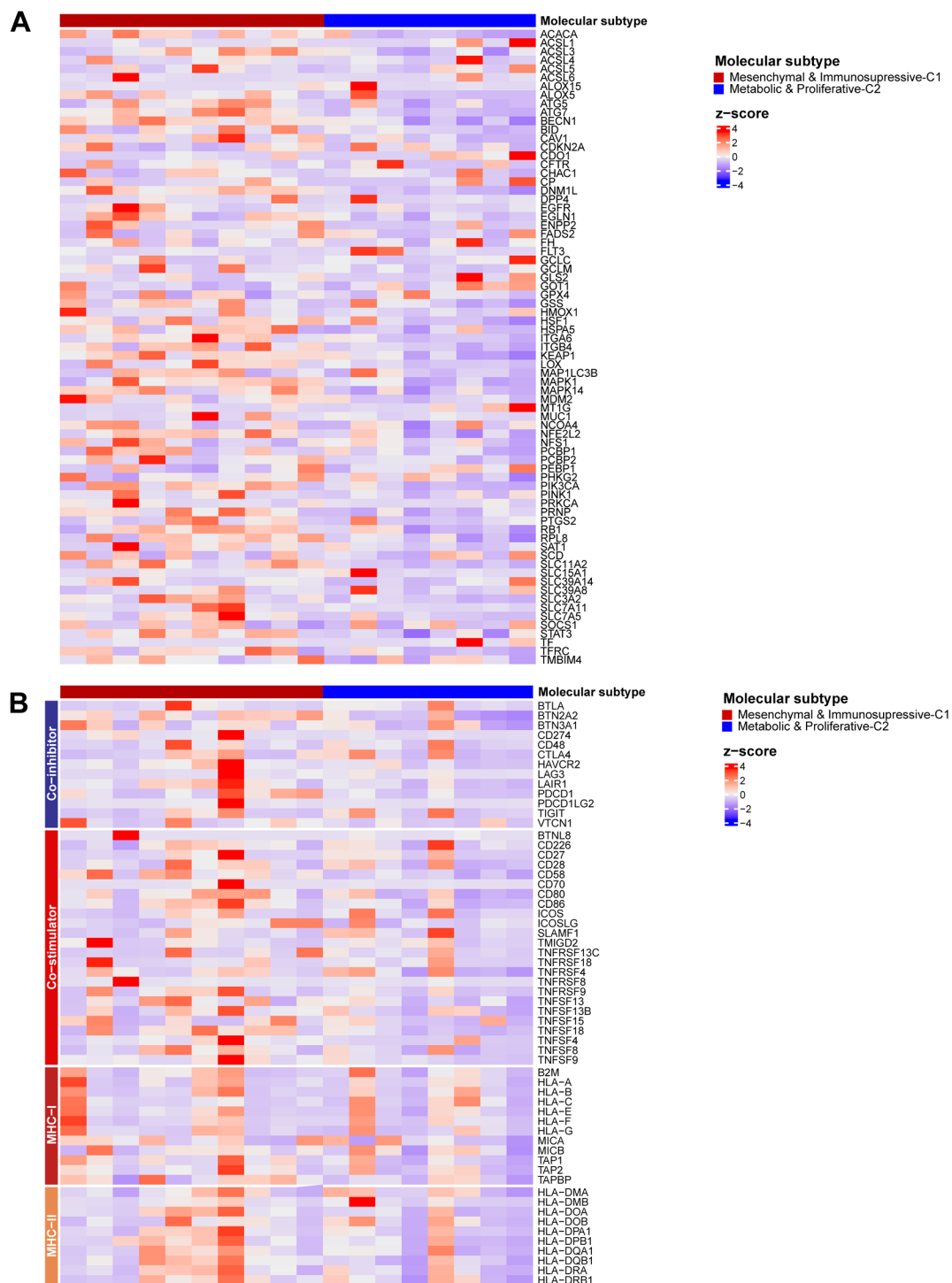
**Supplementary Fig. 8. Validation of ferroptosis-related features and immune escape mechanisms of molecular classes on the verification cohort.** Heatmaps displaying expression levels of **(A)** ferroptosis-related genes; and **(B)** genes encoding co-stimulators, co-inhibitors and MHC

87 antigens in each molecular class. The expression values were normalized and  
88 represented by z-scores. N=274.



**Supplementary Fig. 9. Validation of classifier and molecular classification scheme on the TCGA-CHOL samples. (A)** Heatmap representing the expression of classifier genes in each sample (TCGA-CHOL project, N=36). The expression levels were represented by normalized z-

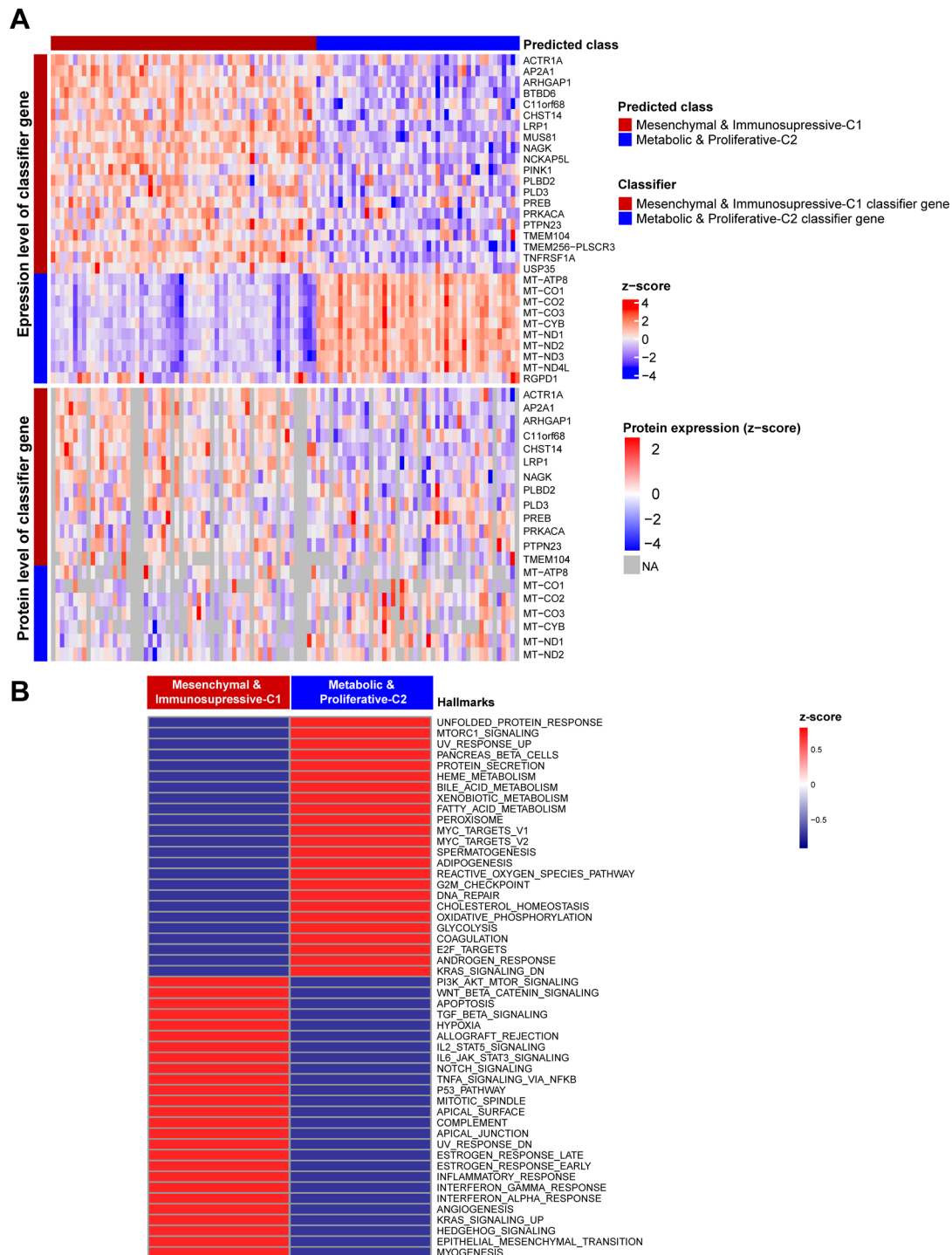
94 scores. The molecular class was predicted by nearest template prediction  
95 (NTP) analysis. **(B)** Heatmap representing the enrichment of hallmark gene  
96 sets in molecular classes for the TCGA-CHOL samples. Single-sample gene  
97 set enrichment analysis (ssGSEA) was used to obtain enrichment scores, with  
98 samples from the same subtype indicated with a normalized z-score.



**Supplementary Fig. 10. Validation of ferroptosis-related features and immune escape mechanisms of molecular classes on the TCGA-CHOL samples.** Heatmaps displaying expression levels of **(A)** ferroptosis-related genes; and **(B)** genes encoding co-stimulators, co-inhibitors and MHC

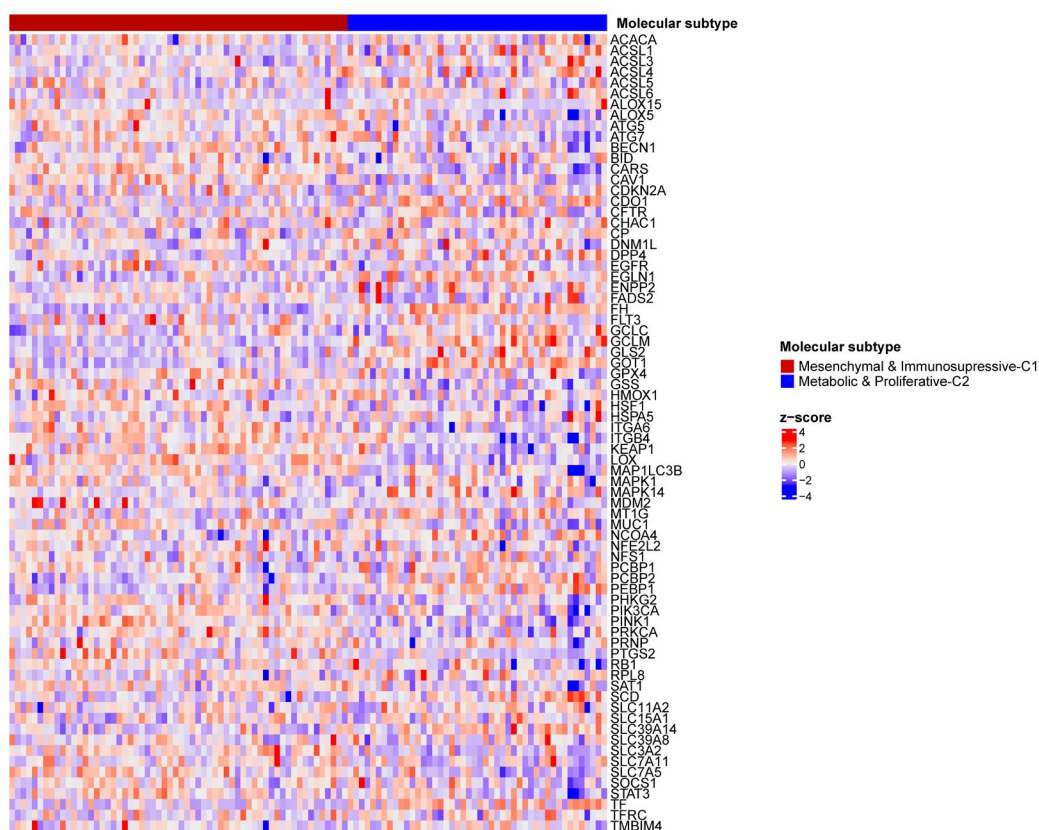
104 antigens in each molecular class. The expression values were normalized and  
105 represented by z-scores.  
106



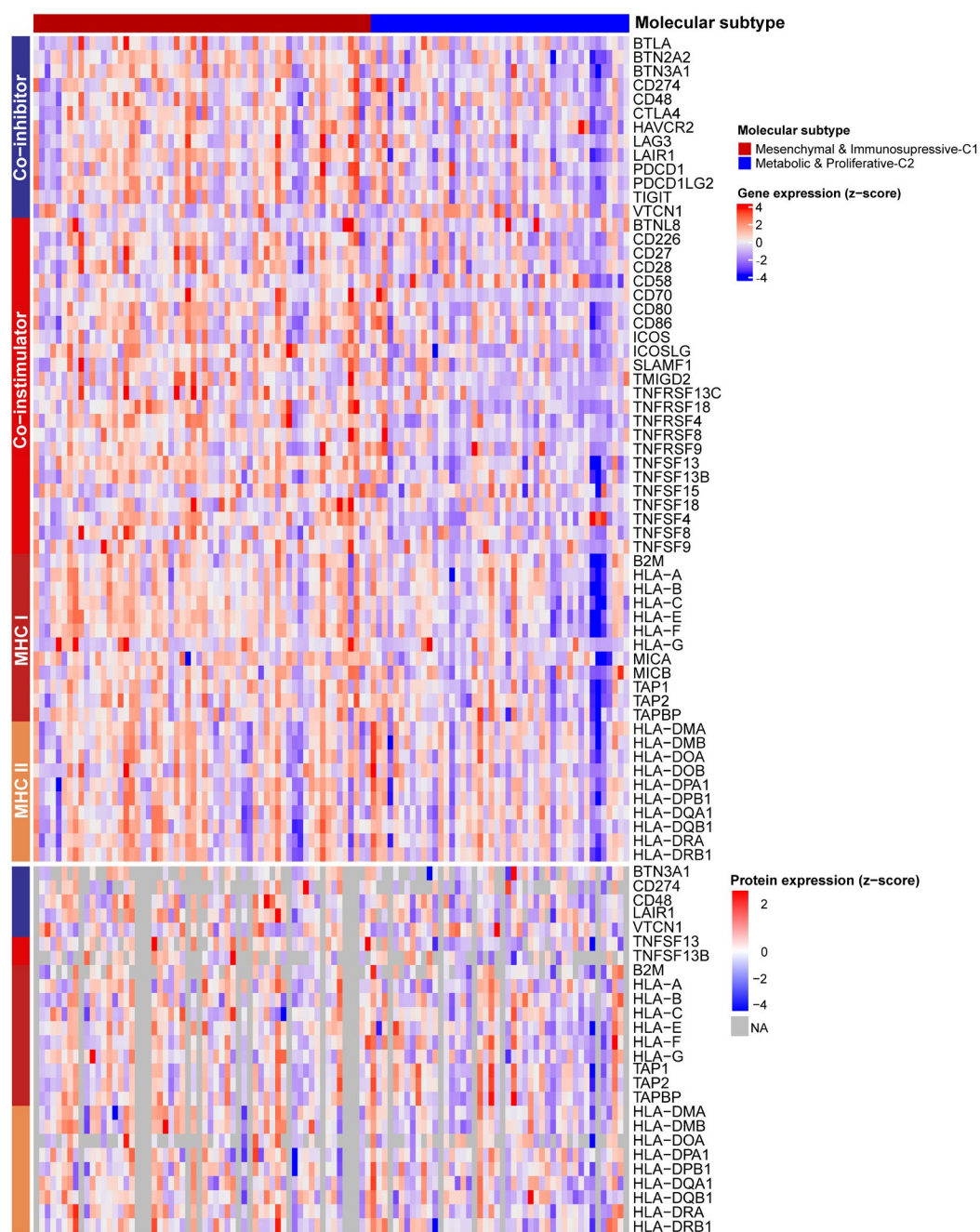


**Supplementary Fig. 11. Validation of classifier and molecular classification scheme on the Dong cohort. (A)** Heatmap representing the RNA and protein expression levels of classifier genes in each sample (Dong cohort, N=255 iCCAs). The RNA and protein expression levels were

represented by normalized z-scores. The molecular class was predicted by nearest template prediction (NTP) analysis. Grey color represents unavailable data (NA). **(B)** Heatmap representing the enrichment of hallmark gene sets in molecular classes for the Dong cohort. Single-sample gene set enrichment analysis (ssGSEA) was used to obtain enrichment scores, with samples from the same subtype indicated with a normalized z-score.



**Supplementary Fig. 12. Validation of ferroptosis-related features of molecular classes on the Dong cohort.** Heatmap displaying expression levels of ferroptosis-related genes in each sample. The expression values were normalized and represented by z-scores.

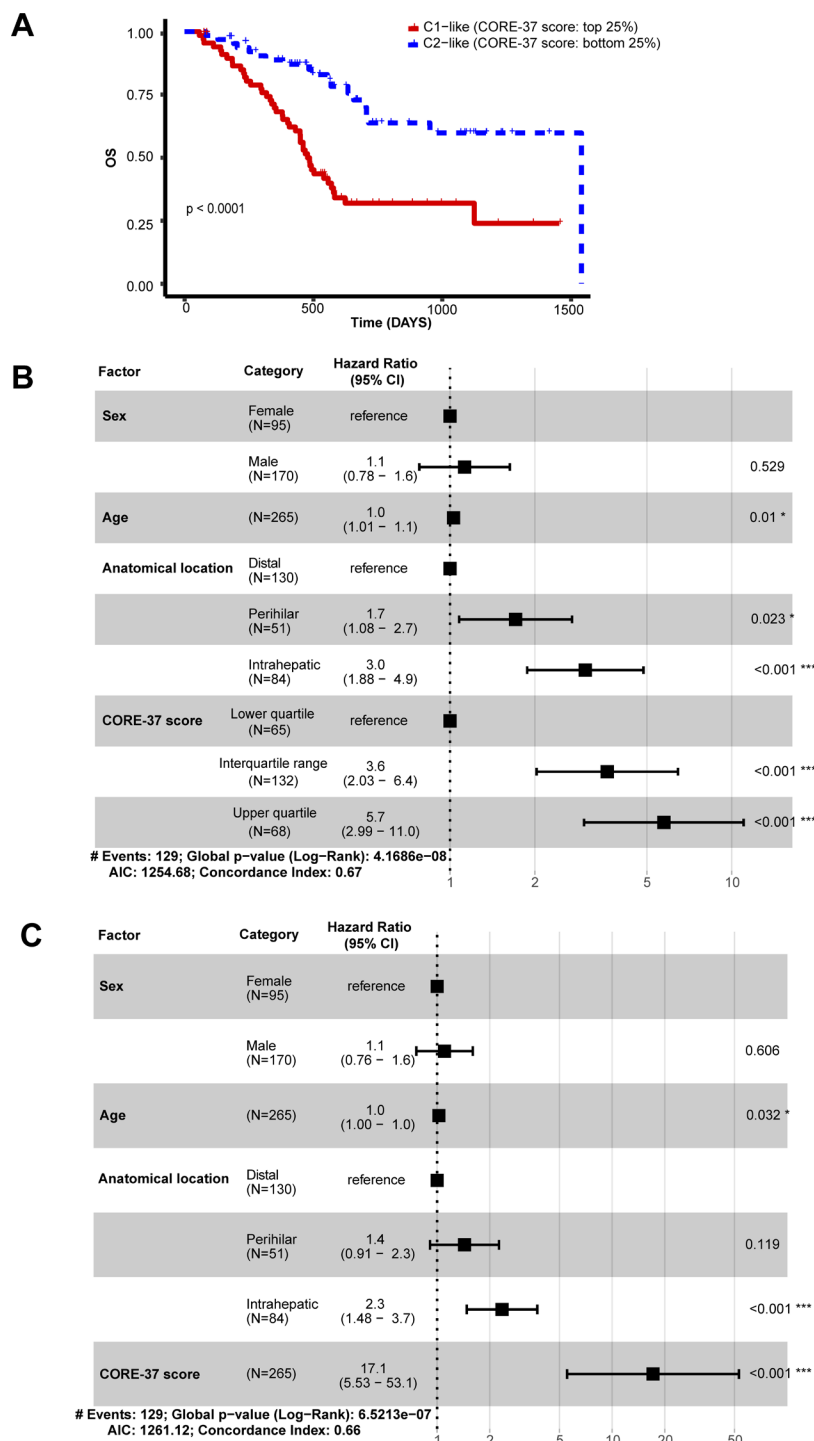


**Supplementary Fig. 13. Validation of immune escape mechanisms of molecular classes on the Dong cohort.** Heatmap displaying RNA and protein expression levels of genes encoding co-stimulators, co-inhibitors and MHC antigens in each molecular class. The expression values were

131 normalized and represented by z-scores. Grey color represents unavailable  
132 data (NA).

133

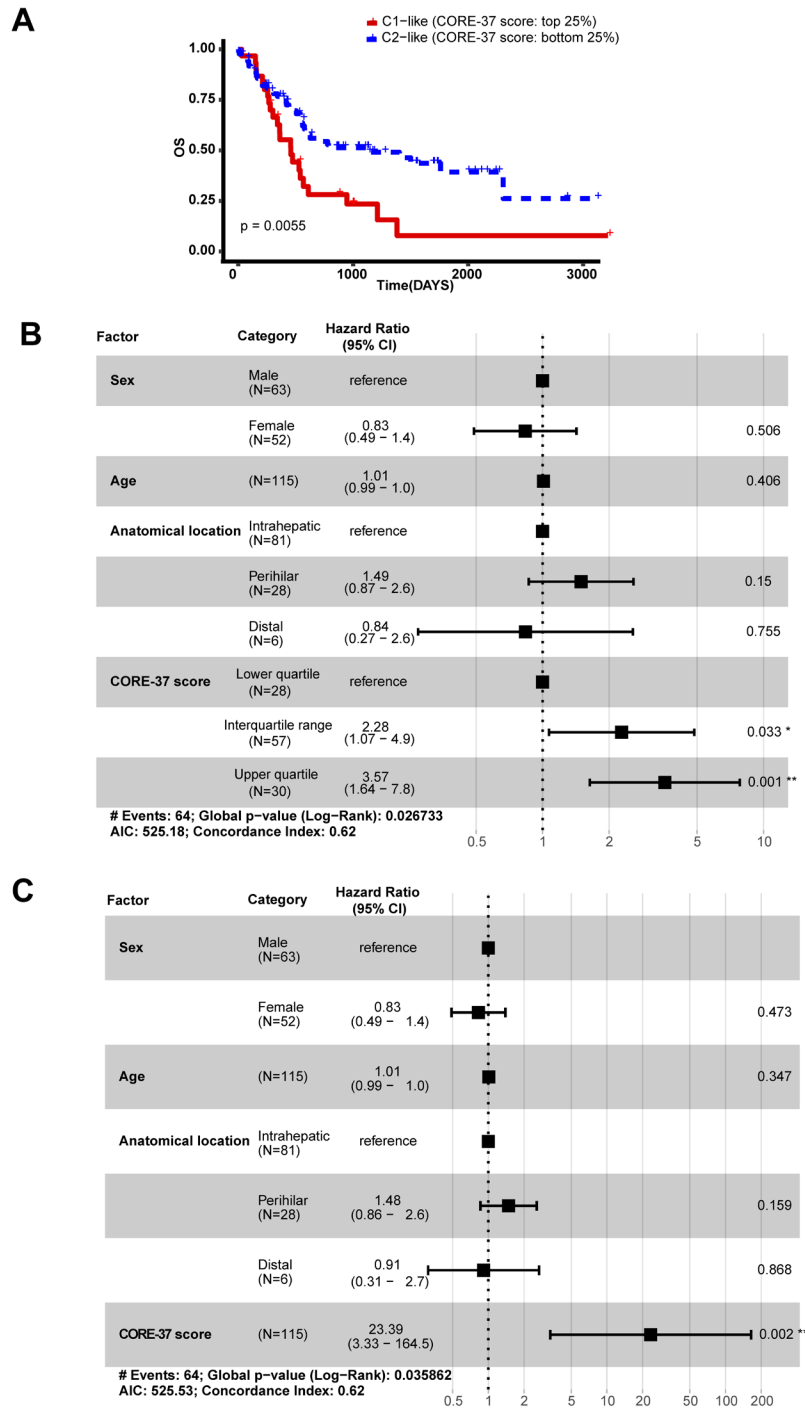
134



**Supplementary Fig. 14. Validation of the developed prognostic indicator on the verification cohort. (A)** Kaplan-Meier curve comparing overall survival (OS) between samples within the top and bottom quartiles of total scores. Forest plots illustrating **(B)** quartile-categorized total score and **(C)**

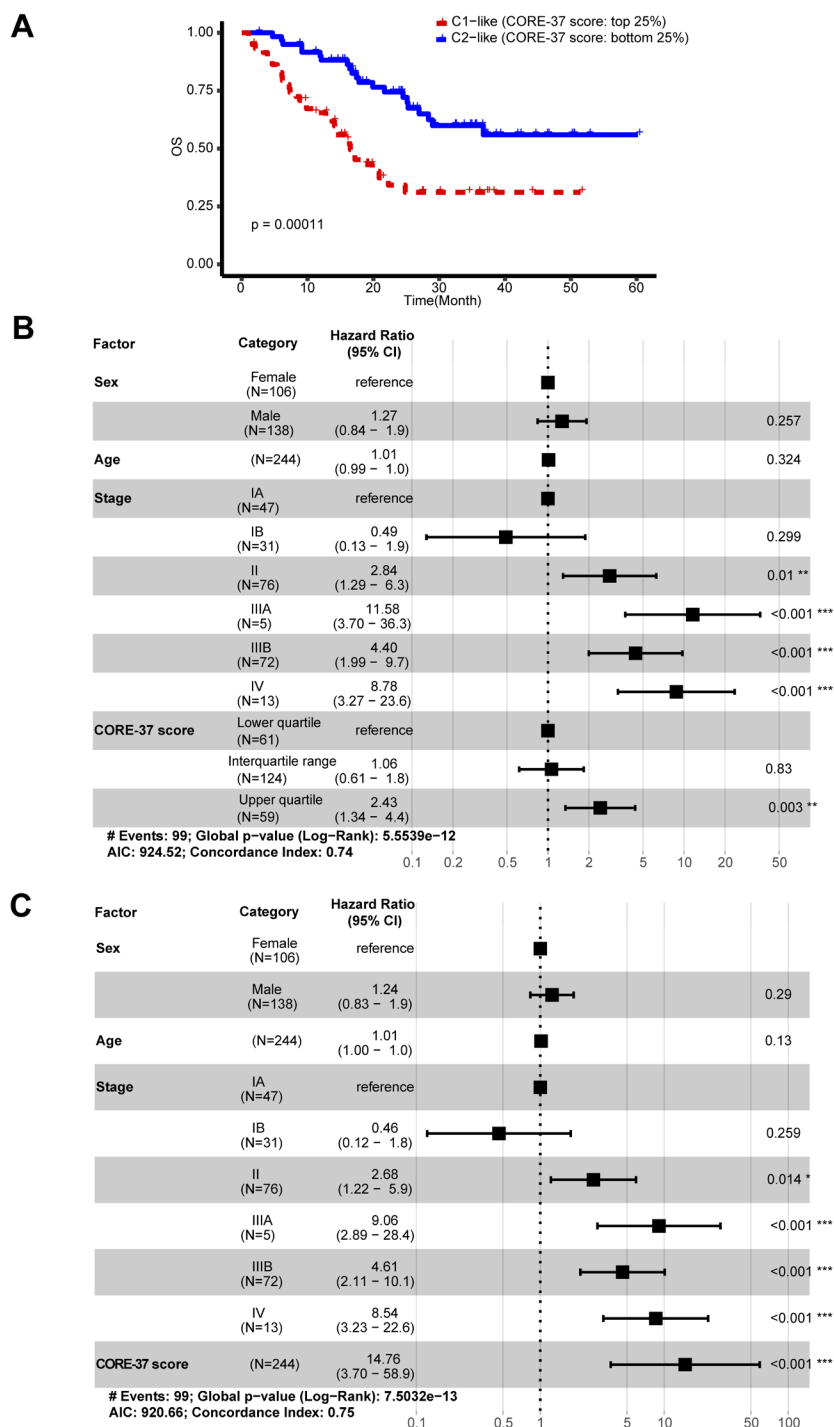
140 continuous total score as independent prognostic indicators, regardless of age,  
141 sex and anatomical location. N=265. *P*-values were calculated by log-rank  
142 test. CI: confidence interval.  
143





**Supplementary Fig. 15. Validation of the developed prognostic indicator on the Jusakul cohort. (A)** Kaplan-Meier curve comparing overall survival (OS) between samples within the top and bottom quartiles of total scores. **(B)** Forest plots illustrating quartile-categorized total score and **(C)** continuous

149 total score as independent prognostic indicators, regardless of age, sex and  
150 anatomical location. N=115. *P*-values were calculated by log-rank test. CI:  
151 confidence interval.  
152



**Supplementary Fig. 16. Validation of the developed prognostic indicator on the Dong cohort. (A)** Kaplan-Meier curve comparing overall survival (OS) between samples within the top and bottom quartiles of total scores. Forest plots illustrating **(B)** quartile-categorized total score and **(C)** continuous total

158 score as independent prognostic indicators, regardless of age, sex and stage.

159 N=244. *P*-values were calculated by log-rank test. CI: confidence interval.

**Supplementary Table 1. Clinical characteristics of CCA patients in the original cohort and stratified cohorts.** Summary for the clinical information of patients or samples included in this study. Purified cohort included the remaining samples after filtrating out samples based on NTP results and overall contamination proportions (verification cohort; **see Material and Methods**).

See the EXCEL file attached.

168 **Supplementary Table 2. Clinical information of 438 samples employed in**  
169 **this study.**

170 See the EXCEL file attached.

171

172 **Supplementary Table 3. Correlation between CCA molecular subtypes**  
173 **and clinical and pathological features (N=438).**

<b>Correlation</b>	<b>Statistical method</b>	<b>p-value</b>
Molecular cluster & Sex	Fisher's Exact Test (two-sided)	0.8
Molecular cluster & Resection	Fisher's Exact Test (two-sided)	<b>0.0001</b>
Molecular cluster & Stage	Fisher's Exact Test (two-sided)	<b>1.00E-07</b>
Molecular cluster & Differentiation	Fisher's Exact Test (two-sided)	0.4335
Molecular cluster & Pathological type	Fisher's Exact Test (two-sided)	0.4
Molecular cluster & Anatomical site	Fisher's Exact Test (two-sided)	<b>1.00E-06</b>
Molecular cluster & Age	Kruskal-Wallis rank sum test	<b>0.006</b>
Molecular cluster & Hepatic contamination	Kruskal-Wallis rank sum test	<b>2.20E-16</b>
Molecular cluster & Pancreatic contamination	Kruskal-Wallis rank sum test	<b>2.20E-16</b>
Molecular cluster & Duodenal contamination	Kruskal-Wallis rank sum test	<b>4.20E-06</b>
Molecular cluster & Lymphatic contamination	Kruskal-Wallis rank sum test	<b>0.0036</b>
Molecular cluster & Neural contamination	Kruskal-Wallis rank sum test	<b>0.0017</b>



174 N=438;  $p < 0.05$  was considered significant and highlighted with **bold** style.

175

176 **Supplementary Table 4. Liver-specific and pancreas-specific gene**  
177 **markers as templates for NTP analysis.**

178 See the EXCEL file attached.

179 Genes were collected at Tissue-specific Gene DataBase in cancer (TissGDB:  
180 <https://bioinfo.uth.edu/TissGDB/>).

181

**Supplementary Table 5. Correlation between CCA molecular subtypes and clinical and pathological features on the purified cohort (N=164).**

Correlation	Statistical method	p-value
molecular cluster & Sex	Fisher's exact test (two-sided)	0.59
molecular cluster & Resection	Fisher's exact test (two-sided)	0.97
molecular cluster & Stage	Fisher's exact test (two-sided)	<b>0.03</b>
molecular cluster & Differentiation degree	Fisher's exact test (two-sided)	0.36
molecular cluster & Pathological type	Fisher's exact test (two-sided)	0.28
molecular cluster & Anatomical location	Fisher's exact test (two-sided)	0.12
molecular cluster & Age	Kruskal-Wallis rank sum test	0.55
molecular cluster & Liver percentage	Kruskal-Wallis rank sum test	<b>0.02</b>
molecular cluster & Pancreas percentage	Kruskal-Wallis rank sum test	0.47
molecular cluster & Duodenum percentage	Kruskal-Wallis rank sum test	NA
molecular cluster & Lymphoid percentage	Kruskal-Wallis rank sum test	0.54
molecular cluster & Neuron percentage	Kruskal-Wallis rank sum test	0.20

N=164;  $p < 0.05$  was considered significant and highlighted with **bold** style.

186 **Supplementary Table 6. Genes selected for the developed molecular**  
187 **classifier.**

188 See the EXCEL file attached.

189 Class Neighbors tool from GenePattern web was used to identify classifier  
190 genes. These were selected based on the dot plot representing signal-to-  
191 noise ratio (SNR) score versus gene rank (**Fig. 5B**).

192     **Supplementary Table 7. The results of NTP analysis.**

193     See the EXCEL file attached.

194

195 **Supplementary Table 8. Differentially expressed genes (DEGs) selected**  
196 **for estimating the prognostic biomarker “Total Score” in each sample.**

197 See the EXCEL file attached.

198 A total of 37 DGEs were involved in the construction of prognostic biomarker,  
199 with the application of “Singscore” R package. The  $p$  values are two-sided and  
200  $p < 0.05$  was considered significant. The  $\log_2$  fold change values and adjusted  
201  $p$ -values ( $p$ -adj) for each gene were listed. N=164.

202

203 **Supplementary Table 9. Net reclassification index comparison between**  
204 **different models.**

Model		control=age + TNM-staging			control=age + TNM-staging		
		new=age+ CORE-37			new= age+ TNM-staging+ CORE-37		
Anatomical location	Item	Estimate	Lower	Upper	Estimate	Lower	Upper
dCCA	NRI	0.171	-0.234	0.550	0.248	-0.031	0.551
	NRI+	0.109	-0.078	0.281	0.146	-0.014	0.291
	NRI-	0.062	-0.193	0.331	0.102	-0.086	0.360
	Pr(Up Case)	0.366	0.163	0.524	0.341	0.090	0.495
	Pr(Down Case)	0.257	0.122	0.395	0.195	0.000	0.364
	Pr(Down Ctrl)	0.331	0.070	0.530	0.302	0.012	0.563
	Pr(Up Ctrl)	0.269	0.147	0.359	0.199	0.021	0.252
pCCA	NRI	0.230	-0.174	0.551	0.196	-0.022	0.630
	NRI+	0.120	-0.133	0.313	0.085	-0.059	0.376
	NRI-	0.111	-0.116	0.271	0.110	-0.013	0.310
	Pr(Up Case)	0.277	0.017	0.495	0.243	0.000	0.535
	Pr(Down Case)	0.158	0.016	0.398	0.158	0.000	0.267
	Pr(Down Ctrl)	0.294	0.044	0.524	0.308	0.000	0.540
	Pr(Up Ctrl)	0.183	0.027	0.362	0.198	0.000	0.291
iCCA	NRI	0.386	-0.168	0.971	0.690	0.185	1.143
	NRI+	0.128	-0.090	0.413	0.274	-0.013	0.514
	NRI-	0.258	-0.160	0.619	0.416	0.153	0.705
	Pr(Up Case)	0.500	0.393	0.652	0.501	0.259	0.706
	Pr(Down Case)	0.372	0.191	0.496	0.227	0.149	0.359
	Pr(Down Ctrl)	0.476	0.305	0.731	0.553	0.277	0.792
	Pr(Up Ctrl)	0.218	0.083	0.491	0.137	0.055	0.226

205 NRI: net reclassification index; Pr: proportion; Ctrl: control; dCCA: distal  
206 cholangiocarcinoma; pCCA: perihilar cholangiocarcinoma; iCCA: intrahepatic  
207 cholangiocarcinoma.  
208



209 **Supplementary Table 10. The raw TPM expression data of 438 samples**

210 **employed in this study.**

211 See the EXCEL file attached.

212